Pergamon

Int. J. Solids Structures Vol. 33, No. 6, pp. 879–897, 1996

0020–7683/96 $9.50 + .00

0020–7683(95)00079–8

A PREDICTOR–CORRECTOR ZIG-ZAG MODEL FOR THE BENDING OF LAMINATED COMPOSITE PLATES

K. H. LEE† and L. CAO
Department of Mechanical and Production Engineering, National University of Singapore, Singapore 0511

(*Received 2 November 1993; in revised form 25 March 1995*)

Abstract — A predictor–corrector approach based on the zig-zag model is proposed for the bending of thick laminated composite plates. The main purpose of the approach is to reduce the differences between the assumed variation of the transverse shear stresses provided by the constitutive equations and the computed variation of the same stresses from the equilibrium equations of elasticity. In the predictor phase, a linear or cubic zig-zag model is adopted and the layerwise polynomial approximation of the transverse shear stresses through the thickness is determined from the equilibrium equations of elasticity. This approximation is then used in a general higher-order zig-zag model in the corrector phase in order to improve the predictions for the displacements and stresses. The present predictor–corrector zig-zag model satisfies the continuity of the in-plane displacements and the transverse shear stresses at the interfaces while maintaining the same number of variables as in Mindlin's theory. The numerical results for the bidirectional bending of both symmetric and antisymmetric thick laminates are in excellent agreement with the exact elasticity results of Pagano. They also show a marked improvement over the results from the linear zig-zag model of Di Sciuva and the cubic zig-zag model of Lee *et al.*, especially at the interfaces.

INTRODUCTION

The use of layerwise displacement models for the analysis of thick laminated composite plates is now widely accepted in research. Such models allow the in-plane displacements to vary in a piecewise manner through the thickness of the laminate and they naturally include the effect of transverse shear deformation. In contrast to the simpler laminatewise displacement models which make use of a single polynomial for the distribution of the in-plane displacements, the layerwise models can reproduce the zig-zag behaviour of the in-plane displacements. This zig-zag behaviour is more pronounced for thick laminates where the transverse shear modulus changes abruptly through the thickness and can be seen in the exact elasticity solutions obtained by Pagano (1970), and Pagano and Hatfield (1972) for the bidirectional bending of rectangular laminated plates. Clearly, it is necessary to use a layerwise model for the analysis of thick laminates in order to predict the in-plane and transverse shear stresses accurately.

Whitney (1969) appears to be the first to employ a layerwise model for improving the gross behaviour of laminates. His model assumed a layerwise quadratic variation of the transverse shear stresses which on integration led to a layerwise cubic variation of the in-plane displacements. Furthermore, by making use of the necessary continuity conditions, the number of variables remained the same as in first-order shear deformation theories (FSDT). However, the equations of equilibrium were taken to be those from the classical lamination theory and are thus not variationally consistent. The numerical results for deflections, natural frequencies and buckling loads were in excellent agreement with available exact elasticity solutions. As no results were given for the in-plane stresses, it was not possible to make any conclusion regarding their accuracy.

In his work, Whitney actually allowed for the possibility of using other than a layerwise quadratic variation of the transverse shear stresses. In principle, a single characterizing function $f(z)$ of the thickness coordinate z was used to generate the layerwise variation

† To whom correspondence should be addressed.

with the condition that the transverse shear stresses be continuous at the interfaces and zero at the free surfaces. For example, he used $f(z) = 1-4(z/h)^2$ to produce the layerwise quadratic variation for his numerical results. Here, h is the total thickness of the laminate. The best results are thus obtained when the function $f(z)$ leads to a layerwise distribution of transverse shear stresses which is close to the exact elasticity solution. Of course, such a function cannot be known *a priori* as it depends not only on the ply configuration but also on the plate geometry, loading and boundary conditions. Also, a single continuous function $f(z)$ may not be sufficient for the description of the distribution of the transverse shear stresses. It should be pointed out here that the use of $f(z)$ was first proposed by Ambartsumyan (1969) for the analysis of homogeneous plates and shells.

Other layerwise or zig-zag models have been presented by Mau (1973), Chou and Carleone (1973), Di Sciuva (1986), Murakami (1986) and Ren (1986). Di Sciuva's model made use of linear piecewise functions and had the advantage of having the same number of variables as the FSDT. In principle, Murakami's model could be extended to higher-order piecewise functions with a further increase in the number of variables. The layerwise cubic model of Ren required two variables more than the FSDT but it produced results which agreed well with those from exact elasticity. These models demonstrated that layerwise functions are necessary for determining the zig-zag thickness distribution of the in-plane displacements.

Reddy (1987) proposed a generalized laminated plate theory which could account for any desired degree of approximation of the distribution of the in-plane displacements through a proper selection of the variables and functions. Reddy also showed that the theory included many of the well known plate theories as special cases. More importantly, the theory can be used in finite elements with Lagrange and Hermite interpolation functions through the laminate thickness. Thus, by increasing the number of variables in a suitable manner, his theory can produce the zig-zag variation of the in-plane displacements.

Recently, Lee *et al.* (1990) presented an improved zig-zag model which has a layerwise cubic variation of the in-plane displacements but the same number of variables as the FSDT. The numerical results for the maximum in-plane stresses at the free surfaces showed very good agreement for the cylindrical bending of thick symmetric cross-ply laminates when compared with the exact elasticity solutions from Pagano (1969). However, the computed displacements and stresses at the interfaces were not accurate enough. The application of the improved zig-zag model to the bidirectional bending of thick symmetric cross-ply laminates in Lee *et al.* (1994) also showed a similar trend. Further investigation showed that the accuracy of the model drops when used for non-symmetric laminates.

The reason for the above inadequacy of the zig-zag model of Lee *et al.* (1990) is very much due to the use of a single parabolic function for the description of the transverse shear stresses in the constitutive equations. As the parabolic function is symmetric with respect to the mid-plane, the performance of the model is best when it is employed for the analysis of symmetric laminates. Of course, the equilibrium equations of elasticity can be used to give an improved distribution of the transverse shear stresses for both symmetric and non-symmetric laminates. However, the differences between the constitutive description and the equilibrium distribution are in fact an indication of possible inaccuracies in the computations of the in-plane displacements and stresses. Although these differences are usually greater for non-symmetric laminates, they can also be significant for symmetric ones and are responsible for the inaccuracies in the displacements and stresses at the interfaces.

The purpose of this paper is thus to present a predictor–corrector approach for the numerical analysis of general thick laminated plates which ensures that the transverse shear stress distributions from both constitutive and equilibrium considerations are sufficiently close to each other before the computations of the displacements and stresses are considered sufficiently accurate. In the predictor phase, the linear zig-zag model of Di Sciuva (1986) or the cubic zig-zag model of Lee *et al.* (1990) can be adopted. Thereafter, a general higher-order zig-zag model based on the previous equilibrium distribution of the transverse shear stresses is utilized in the corrector phase. The advantage of the present approach is that a high level of accuracy can be achieved with the same number of variables as in the FSDT even though a general higher-order zig-zag model is employed in the corrector phase.

When the model used in the predictor phase is a simple one, the corrector phase can, of course, be performed analytically to yield a higher-order refined theory with an increase in the number of variables. For example, Reddy *et al.* (1991) derived a variationally consistent layerwise cubic model for symmetric laminates starting from the simple classical lamination theory (CLT). The model has five variables (four more than the CLT) and performed very well in comparison with the exact elasticity solutions from Pagano. As it does not consider the deformation of the mid-plane, this model actually has two variables more than the layerwise cubic model of Lee *et al.* (1990). This increase in the number of variables, especially for non-symmetric laminates, is the primary reason for not deriving higher-order refined theories analytically from other than the CLT. The present paper serves to address this problem by providing a predictor-corrector approach in numerical form so that the model used in the predictor phase is not limited to the CLT.

Noor and Burton (1989), Noor and Peters (1989) and Noor *et al.* (1990, 1991) have proposed two predictor–corrector procedures for the accurate prediction of the global and detailed response characteristics of multilayered plates and shells. Both procedures used the FSDT in the predictor phase. In the first procedure, the three-dimensional equilibrium equations and constitutive relations were used to determine *a posteriori* estimates for the composite shear correction factors. The improved shear correction factors were then employed for adjusting the transverse shear stiffnesses in order to obtain more accurate results. In the other procedure, the functional dependence of the displacement components on the thickness coordinate was calculated *a posteriori* in the corrector phase. The corrected quantities were then used in conjunction with the three-dimensional equations to provide better estimates for the different response quantities. While the numerical results from both procedures agreed well with exact elasticity results, the second one generally gave better predictions. However, the second procedure was more involved as it required the use of the Rayleigh–Ritz technique in conjunction with the Principle of Minimum Potential Energy for the determination of the 12 unknown parameters in the symmetric and antisymmetric functions of the thickness coordinate.

The predictor–corrector approach described in this paper does not depend on the calculation of improved shear correction factors nor on an increase in the number of variables from five in the FSDT to 12 in the Rayleigh–Ritz technique mentioned above. Instead, by using a layerwise model which satisfies the continuity of the in-plane displacements and the transverse shear stresses at the interfaces, the number of variables is kept the same as in the FSDT. Essentially, the distribution of the transverse shear stresses obtained from the equilibrium equations of elasticity in the predictor phase is used to control the layerwise description of the displacements in the corrector phase. For this purpose, a linear or cubic zig-zag model is employed in the predictor phase while a general higher-order zig-zag model is utilized in the corrector phase.

In this paper, the salient features of the general higher-order zig-zag model are described first. Following this, the predictor-corrector procedure is presented and then applied to the benchmark problems of Pagano (1970), and Pagano and Hatfield (1972). The numerical results from this predictor–corrector zig-zag model for the bidirectional bending of both symmetric and antisymmetric thick laminates are compared with those from exact elasticity, the linear zig-zag model of Di Sciuva (1986) and the cubic zig-zag model of Lee *et al.* (1990).

THEORY

Consider a laminated composite plate of uniform thickness h with n orthotropic layers (Fig. 1). The x–y plane is taken to be the mid-plane of the laminate, and the principal material axes of elasticity can in general be oriented at an angle to the laminate axes. As usual, by assuming a state of plane stress, the reduced plane stress constitutive equations for a particular layer expressed in terms of stresses and strains in the laminate axes are

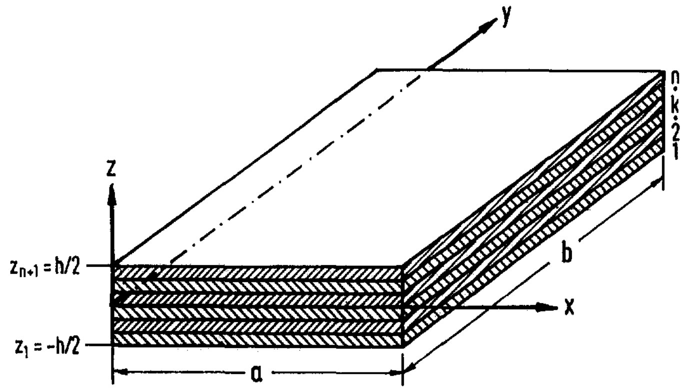

Fig. 1. Laminate geometry.

$$\begin{bmatrix} \sigma_1 \\ \sigma_2 \\ \sigma_6 \end{bmatrix} = \begin{bmatrix} Q_{11} & Q_{12} & Q_{16} \\ Q_{12} & Q_{22} & Q_{26} \\ Q_{16} & Q_{26} & Q_{66} \end{bmatrix} \begin{bmatrix} \varepsilon_1 \\ \varepsilon_2 \\ \varepsilon_6 \end{bmatrix}$$

$$\begin{bmatrix} \sigma_4 \\ \sigma_5 \end{bmatrix} = \begin{bmatrix} Q_{44} & Q_{45} \\ Q_{45} & Q_{55} \end{bmatrix} \begin{bmatrix} \varepsilon_4 \\ \varepsilon_5 \end{bmatrix}, \tag{1}$$

where Q_{ij} are the transformed reduced elastic constants.

In the present model, the layerwise displacement field is written in the general form as

$$\begin{aligned} u^k &= u_0^k - zw_{,x} + f_x^k(z)\phi_x^k \\ v^k &= v_0^k - zw_{,y} + f_y^k(z)\phi_y^k \\ w^k &= w \quad (k = 1, \ldots, n), \end{aligned} \tag{2}$$

where u_0^k, v_0^k, ϕ_x^k, ϕ_y^k and w are functions of the x and y coordinates, with the superscript k referring to the kth layer. The variables u_0^k and v_0^k can be interpreted as the in-plane displacements on the x–y plane (that is, at $z = 0$) if the displacement distributions u^k and v^k for the kth layer are extrapolated to the x–y plane. Similarly, the variables ϕ_x^k and ϕ_y^k are the transverse shear strains at $z = 0$ if the transverse shear strain distributions ε_5^k and ε_4^k for the kth layer are extrapolated to the x–y plane provided the coefficient of z in the polynomials $f_x^k(z)$ and $f_y^k(z)$ is unity.

It is noted that the introduction of the general polynomials $f_x^k(z)$ and $f_y^k(z)$ allows the transverse shear strains to vary in an arbitrary manner through the thickness of each layer. Of course, this is subject to the condition that they enable the satisfaction of zero values at the free surfaces. From this point of view, the linear and cubic layerwise models of Di Sciuva (1986) and Lee *et al.* (1990) are special cases of the above displacement model. In common with all higher-order theories for the bending of plates, no shear correction factors are required here.

As a first step towards a reduction in the number of variables in the model, the continuity of the transverse shear stresses σ_5 and σ_4 at the interfaces is imposed. By making use of the constitutive relations in eqns (1), this condition gives rise to the following recurrence relations for ϕ_x^k and ϕ_y^k for generally orthotropic layers:

$$\begin{aligned} \phi_x^k &= a_k' \phi_x^{k-1} + b_k' \phi_y^{k-1} \\ \phi_y^k &= c_k' \phi_x^{k-1} + d_k' \phi_y^{k-1}, \end{aligned} \tag{3}$$

where the coefficients a_k', b_k', c_k' and d_k' for each layer are given by

$$
\begin{aligned}
a'_k &= \frac{f^{k-1}_{x,z}(z_k)}{f^k_{x,z}(z_k)} \frac{Q^k_{44}Q^{k-1}_{55} - Q^k_{45}Q^{k-1}_{45}}{A^k} \\
b'_k &= \frac{f^{k-1}_{y,z}(z_k)}{f^k_{x,z}(z_k)} \frac{Q^k_{44}Q^{k-1}_{45} - Q^k_{45}Q^{k-1}_{44}}{A^k} \\
c'_k &= \frac{f^{k-1}_{x,z}(z_k)}{f^k_{y,z}(z_k)} \frac{Q^k_{55}Q^{k-1}_{45} - Q^k_{45}Q^{k-1}_{55}}{A^k} \\
d'_k &= \frac{f^{k-1}_{y,z}(z_k)}{f^k_{y,z}(z_k)} \frac{Q^k_{55}Q^{k-1}_{44} - Q^k_{45}Q^{k-1}_{45}}{A^k}
\end{aligned} \tag{4}
$$

and

$$
A^k = Q^k_{44}Q^k_{55} - Q^k_{45}Q^k_{45}. \tag{5}
$$

In the above equations, z_j is the z-coordinate of the lower surface of the jth layer, and $f^k_{i,z}(z)$ denotes the derivative of $f^k_i(z)$ with respect to z. By applying the recurrence relations (3) successively, ϕ^k_x and ϕ^k_y can be expressed explicitly in terms of ϕ^1_x and ϕ^1_y as

$$
\begin{aligned}
\phi^k_x &= a_k\phi^1_x + b_k\phi^1_y \\
\phi^k_y &= c_k\phi^1_x + d_k\phi^1_y,
\end{aligned} \tag{6}
$$

where a_k, b_k, c_k and d_k can be written as products of a'_k, b'_k, c'_k and d'_k. The first layer has been chosen as the reference layer for the sake of simplicity.

The next step is to obtain the expressions for u^k_0 and v^k_0 in terms of the variables u^1_0, v^1_0, ϕ^1_x and ϕ^1_y by satisfying the continuity of the in-plane displacements at the interfaces. This yields the following equations:

$$
\begin{aligned}
u^k_0 &= u^1_0 + \alpha_k\phi^1_x + \beta_k\phi^1_y \\
v^k_0 &= v^1_0 + \gamma_k\phi^1_x + \eta_k\phi^1_y,
\end{aligned} \tag{7}
$$

where, for $k = 2, \ldots, n$

$$
\begin{aligned}
\alpha_k &= \sum_{j=2}^{k} [f^{j-1}_x(z_j)a_{j-1} - f^j_x(z_j)a_j] \\
\beta_k &= \sum_{j=2}^{k} [f^{j-1}_x(z_j)b_{j-1} - f^j_x(z_j)b_j] \\
\gamma_k &= \sum_{j=2}^{k} [f^{j-1}_y(z_j)c_{j-1} - f^j_y(z_j)c_j] \\
\eta_k &= \sum_{j=2}^{k} [f^{j-1}_y(z_j)d_{j-1} - f^j_y(z_j)d_j].
\end{aligned} \tag{8}
$$

By substituting eqns (6) and (7) for u^k_0, v^k_0, ϕ^k_x and ϕ^k_y into eqns (2), it is seen that the final displacement field for an n-layer laminate contains only five variables, namely, $u^1_0, v^1_0, \phi^1_x, \phi^1_y$ and w. This final layerwise displacement field is given by

$$
\begin{aligned}
u^k &= u^1_0 - zw_{,x} + p_k(z)\phi^1_x + q_k(z)\phi^1_y \\
v^k &= v^1_0 - zw_{,y} + r_k(z)\phi^1_x + s_k(z)\phi^1_y \\
w^k &= w \quad (k = 1, \ldots, n),
\end{aligned} \tag{9}
$$

where

$$
\begin{aligned}
p_k(z) &= \alpha_k + a_k f_x^k(z) \\
q_k(z) &= \beta_k + b_k f_x^k(z) \\
r_k(z) &= \gamma_k + c_k f_y^k(z) \\
s_k(z) &= \eta_k + d_k f_y^k(z).
\end{aligned}
\tag{10}
$$

It is important to note that the linear zig-zag model can be recovered from the above displacement field by specifying $f_x^k(z) = f_y^k(z) = z$ for all k. Similarly, the cubic model is obtained by letting $f_x^k(z) = f_y^k(z) = (z - 4z^3/3h^2)$. In fact, in the present predictor–corrector approach, one of these two models is used in the predictor phase in order to provide the polynomial functions $f_x^k(z)$ and $f_y^k(z)$ for all the layers in the corrector phase.

The governing equations corresponding to the final displacement field are derived using the Principle of Virtual Work. These variationally consistent equations are

$$
\begin{aligned}
\delta u_0^1 &: \frac{\partial N_1}{\partial x} + \frac{\partial N_6}{\partial y} = 0 \\
\delta v_0^1 &: \frac{\partial N_6}{\partial x} + \frac{\partial N_2}{\partial y} = 0 \\
\delta \phi_x^1 &: \frac{\partial P_1}{\partial x} + \frac{\partial P_{61}}{\partial y} - R_1 = 0 \\
\delta \phi_y^1 &: \frac{\partial P_{62}}{\partial x} + \frac{\partial P_2}{\partial y} - R_2 = 0 \\
\delta w &: \frac{\partial^2 M_1}{\partial x^2} + 2\frac{\partial^2 M_6}{\partial x \partial y} + \frac{\partial^2 M_2}{\partial y^2} + q = 0,
\end{aligned}
\tag{11}
$$

where q is the distributed transverse load, and the stress resultants are given by

$$
\begin{aligned}
N_i &= \sum_{k=1}^{n} \int_{z_k}^{z_{k+1}} \sigma_i^k \,\mathrm{d}z \quad (i = 1, 2, 6) \\
M_i &= \sum_{k=1}^{n} \int_{z_k}^{z_{k+1}} z\sigma_i^k \,\mathrm{d}z \quad (i = 1, 2, 6) \\
P_1 &= \sum_{k=1}^{n} \int_{z_k}^{z_{k+1}} (p_k(z)\sigma_1^k + r_k(z)\sigma_6^k)\,\mathrm{d}z \\
P_2 &= \sum_{k=1}^{n} \int_{z_k}^{z_{k+1}} (q_k(z)\sigma_6^k + s_k(z)\sigma_2^k)\,\mathrm{d}z \\
P_{61} &= \sum_{k=1}^{n} \int_{z_k}^{z_{k+1}} (p_k(z)\sigma_6^k + r_k(z)\sigma_2^k)\,\mathrm{d}z \\
P_{62} &= \sum_{k=1}^{n} \int_{z_k}^{z_{k+1}} (q_k(z)\sigma_1^k + s_k(z)\sigma_6^k)\,\mathrm{d}z
\end{aligned}
$$

$$R_1 = \sum_{k=1}^{n} \int_{z_k}^{z_{k+1}} (a_k f^{\prime k}_{x,z}(z)\sigma_5^k + c_k f^{\prime k}_{y,z}(z)\sigma_4^k)\, dz$$

$$R_2 = \sum_{k=1}^{n} \int_{z_k}^{z_{k+1}} (b_k f^{\prime k}_{x,z}(z)\sigma_5^k + d_k f^{\prime k}_{y,z}(z)\sigma_4^k)\, dz. \tag{12}$$

The Principle of Virtual Work also provides the boundary conditions which for a smooth boundary are given by specifying

$$\begin{aligned}
u_{0n}^1 &\quad \text{or} \quad N_n \\
v_{0n}^1 &\quad \text{or} \quad N_{ns} \\
w &\quad \text{or} \quad \frac{\partial M_n}{\partial n} + 2\frac{\partial M_{ns}}{\partial s} \\
\frac{\partial w}{\partial n} &\quad \text{or} \quad M_n \\
\phi_n^1 &\quad \text{or} \quad P_n \\
\phi_{ns}^1 &\quad \text{or} \quad P_{ns},
\end{aligned} \tag{13}$$

where the subscripts n and s refer to the normal and tangential directions, respectively, to the boundary of the plate. At discontinuities, the corner conditions are

$$w \quad \text{or} \quad M_{ns}. \tag{14}$$

Expressed in terms of the displacements, the governing equations can be written as

$$\mathbf{Lu} = \mathbf{q}, \tag{15}$$

where $\mathbf{L}$ is the differential operator matrix, and $\mathbf{u}$ and $\mathbf{q}$ are the generalized displacement and load vectors given by

$$\begin{aligned}
\mathbf{u} &= [u_0^1 \quad v_0^1 \quad \phi_x^1 \quad \phi_y^1 \quad w]^T \\
\mathbf{q} &= [0 \quad 0 \quad 0 \quad 0 \quad q]^T.
\end{aligned} \tag{16}$$

Instead of using the variables $u_0^1, v_0^1, \phi_x^1, \phi_y^1$ and w, the governing equations and boundary conditions can be written in terms of $u_0^m, v_0^m, \phi_x^m, \phi_y^m$ and w, where the superscript m refers to the mid-plane of the laminate. This can be performed through a simple transformation.

PREDICTOR-CORRECTOR APPROACH

Predictor phase

In the predictor phase, the linear or cubic zig-zag model is used to provide the initial estimate of $\mathbf{u}$ from which the in-plane stresses σ_1, σ_2 and σ_6 can be found. For most problems, the initial estimate from the linear zig-zag model is sufficient and can be obtained from the general higher-order model by setting

$$f_x^{\prime k}(z) = f_y^{\prime k}(z) = z \quad (k = 1, \ldots, n). \tag{17}$$

If a better estimate is required, the cubic zig-zag model is used by letting

$$f_x^k(z) = f_y^k(z) = z - \frac{4z^3}{3h^2} \quad (k = 1, \ldots, n). \tag{18}$$

Using the results from one of the two models, the transverse shear stresses σ_5 and σ_4 are calculated by integrating the three-dimensional equilibrium equations in the thickness direction. In the absence of body forces, these are

$$\sigma_5^k(z) = -\sum_{i=1}^{k-1} \int_{z_i}^{z_{i+1}} (\sigma_{1,x}^i(z) + \sigma_{6,y}^i(z))\,\mathrm{d}z - \int_{z_k}^{z} (\sigma_{1,x}^k(z) + \sigma_{6,y}^k(z))\,\mathrm{d}z$$

$$\sigma_4^k(z) = -\sum_{i=1}^{k-1} \int_{z_i}^{z_{i+1}} (\sigma_{6,x}^i(z) + \sigma_{2,y}^i(z))\,\mathrm{d}z - \int_{z_k}^{z} (\sigma_{6,x}^k(z) + \sigma_{2,y}^k(z))\,\mathrm{d}z. \tag{19}$$

Corrector phase

In the corrector phase, the transverse shear stress distribution found earlier is used to determine the new polynomial functions $f_x^k(z)$ and $f_y^k(z)$ in the layerwise displacement field. To do this, let the functions be represented as a power series by

$$f_x^k(z) = \sum_{j=1}^{m+1} g_j^k z^j \quad (k = 1, \ldots, n \text{ and } g_1^k = 1)$$

$$f_y^k(z) = \sum_{j=1}^{m+1} h_j^k z^j \quad (k = 1, \ldots, n \text{ and } h_1^k = 1), \tag{20}$$

where g_j^k and h_j^k are the coefficients for the jth power of z associated with the two in-plane displacements of the kth layer. Without loss in generality, the values of g_1^k and h_1^k are taken to be unity so that the variables ϕ_x^k and ϕ_y^k denote the transverse shear strains at $z = 0$ on extrapolation of the transverse shear strain distributions ε_5^k and ε_4^k for the kth layer to the x–y plane. By making use of the constitutive relations in eqns (1), the transverse shear stresses σ_5 and σ_4 are given by

$$\sigma_5^k(z) = \sum_{j=0}^{m} g_{j+1}^k (j+1) z^j Q_{55}^k \phi_x^k + \sum_{j=0}^{m} h_{j+1}^k (j+1) z^j Q_{45}^k \phi_y^k$$

$$\sigma_4^k(z) = \sum_{j=0}^{m} g_{j+1}^k (j+1) z^j Q_{45}^k \phi_x^k + \sum_{j=0}^{m} h_{j+1}^k (j+1) z^j Q_{44}^k \phi_y^k. \tag{21}$$

Evidently, the coefficients g_j^k and h_j^k must be chosen such that the transverse shear stress distributions given by both eqns (19) and (21) are coincident. One way is to express eqns (19) explicitly in powers of z so that g_j^k and h_j^k can be deduced from a comparison with eqns (21). This method is convenient when only one corrector phase is desired because the number of terms $m+1$ used to represent $f_x^k(z)$ and $f_y^k(z)$ is only two greater than the order of the zig-zag model in the predictor phase. For instance, if the linear model is used, then three terms are needed. However, the method grows in complexity with subsequent corrector phases because of the increase in the number of terms.

A more general procedure is to fix the number of terms used in the power series for $f_x^k(z)$ and $f_y^k(z)$ in all the corrector phases. Usually, five terms are more than sufficient. The distributions given by eqns (19) are then approximated by the same number of terms even though the exact representation requires two more. In order to provide a good approximation, Chebyshev polynomials are used for the distributions from eqns (19) since they converge much more rapidly over the interval than the corresponding power series due to their orthogonality. To obtain the expansions for $\sigma_5^k(z)$ and $\sigma_4^k(z)$ in terms of Chebyshev polynomials, a change in variable is first made for each of the layers by writing

$$z = \frac{z_{k+1}+z_k}{2} + \frac{z_{k+1}-z_k}{2}\eta \tag{22}$$

so that the interval $[z_k, z_{k+1}]$ becomes $[-1, +1]$. With this transformation, $\sigma_5^k(z)$ and $\sigma_4^k(z)$ for each layer can be expressed as

$$\sigma_5^k(\eta) = \tfrac{1}{2}E_0^k + \sum_{j=1}^{m} E_j^k T_j(\eta)$$

$$\sigma_4^k(\eta) = \tfrac{1}{2}F_0^k + \sum_{j=1}^{m} F_j^k T_j(\eta), \tag{23}$$

where $T_j(\eta)$ is the jth Chebyshev polynomial in terms of η, and the coefficients E_j^k and F_j^k are given by

$$E_j^k = \frac{2}{\pi}\int_{-1}^{+1} \sigma_5^k(\eta)\frac{T_j(\eta)}{\sqrt{1-\eta^2}}\,d\eta$$

$$F_j^k = \frac{2}{\pi}\int_{-1}^{+1} \sigma_4^k(\eta)\frac{T_j(\eta)}{\sqrt{1-\eta^2}}\,d\eta. \tag{24}$$

These coefficients can be found by performing the integration numerically. Once they are found, the Chebyshev expansion is transformed to a power series in terms of η through an appropriate summation of the coefficients. The resulting power series in η is then converted into a power series in z so that $\sigma_5^k(z)$ and $\sigma_4^k(z)$ can be expressed finally as

$$\sigma_5^k(z) = \sum_{j=0}^{m} G_j^k z^j$$

$$\sigma_4^k(z) = \sum_{j=0}^{m} H_j^k z^j. \tag{25}$$

For the transverse shear stress distributions given by eqns (21) and (25) to be the same, it is obvious that the coefficients g_j^k and h_j^k in the functions $f_x^k(z)$ and $f_y^k(z)$ for the in-plane displacements must be given by

$$g_{j+1}^k = \frac{G_j^k Q_{44}^k - H_j^k Q_{45}^k}{(j+1)A^k\phi_x^k}$$

$$h_{j+1}^k = \frac{H_j^k Q_{55}^k - G_j^k Q_{45}^k}{(j+1)A^k\phi_y^k}, \tag{26}$$

where A^k has already been defined earlier in eq. (5). Now, the fact that g_1^k and h_1^k have been taken as unity in eqns (20) demands that

$$A^k\phi_x^k = G_0^k Q_{44}^k - H_0^k Q_{45}^k$$

$$A^k\phi_y^k = H_0^k Q_{55}^k - G_0^k Q_{45}^k. \tag{27}$$

Combining eqns (26) and (27) yields

$$g^k_{j+1} = \frac{1}{(j+1)} \frac{G^k_j Q^k_{44} - H^k_j Q^k_{45}}{G^k_0 Q^k_{44} - H^k_0 Q^k_{45}}$$

$$h^k_{j+1} = \frac{1}{(j+1)} \frac{H^k_j Q^k_{55} - G^k_j Q^k_{45}}{H^k_0 Q^k_{55} - G^k_0 Q^k_{45}}. \quad (28)$$

It is observed that the use of the above expressions for g^k_j and h^k_j in the corrector phase preserves the shapes but not the actual magnitudes of the products $f^k_x(z)\phi^k_x$ and $f^k_y(z)\phi^k_y$. This is because the variables ϕ^k_x and ϕ^k_y are treated as new unknowns to be solved for in the corrector phase.

The corrector phase is completed by making use of the new polynomial functions $f^k_x(z)$ and $f^k_y(z)$ in the layerwise displacement field of eqns (2). This gives rise to a new differential operator matrix **L** which is different by a small amount from the old one in two rows and columns. At this point, either a fresh solution or a modified solution can be obtained, with the latter made available through standard re-analysis techniques.

NUMERICAL RESULTS

The effectiveness of the proposed predictor–corrector approach is assessed by applying it to five problems involving the bidirectional bending of thick simply-supported symmetric and antisymmetric specially orthotropic laminates subjected to sinusoidal loading. The three-dimensional exact elasticity solutions provided by Pagano (1970), and Pagano and Hatfield (1972) for these problems are used as the benchmark for quantifying the accuracy of the present method. For the purpose of comparison with other layerwise or zig-zag theories which have the same number of variables, results from Di Sciuva's linear theory (DST) and Lee *et al.*'s cubic theory (LT) are also presented. The results from the DST have been calculated independently (without any shear correction factor) by using eqns (17) in the present general higher-order zig-zag model whereas the results from the LT (except for the first problem) are available from Lee *et al.* (1994). Alternatively, the latter results can be obtained independently by using eqns (18) in the present model.

The five problems which are studied here are

(1) an antisymmetric two-layer (0°/90°) cross-ply square laminate ($a = b$) with layers of equal thickness,
(2) a symmetric three-layer (0°/90°/0°) cross-ply square laminate ($a = b$) with layers of equal thickness,
(3) the same lamination geometry as in (2) but with $b = 3a$,
(4) a symmetric four-layer (0°/90°/90°/0°) cross-ply square laminate ($a = b$) with layers of equal thickness, and
(5) a symmetric five-layer (0°/90°/0°/90°/0°) cross-ply square laminate ($a = b$) with layers at the same orientation of equal thickness and with the total thickness of the 0° and 90° layers the same.

In all the problems, the material constants for each orthotropic layer are assumed to be $E_L = 25E_T$, $G_{LT} = 0.5E_T$, $G_{TT} = 0.2E_T$ and $\nu_{LT} = \nu_{TT} = 0.25$, where L and T denote the directions parallel and perpendicular to the direction of the fibre orientation, respectively. The laminate, which has edge lengths a and b in the x and y directions, respectively, is assumed to have the following simply supported conditions:

$$v^1_0 = w = \phi^1_y = N_x = M_x = P_x = 0 \quad \text{at} \quad x = (0, a)$$

$$u^1_0 = w = \phi^1_x = N_y = M_y = P_y = 0 \quad \text{at} \quad y = (0, b). \quad (29)$$

Under the above boundary conditions and the sinusoidal transverse load given by

$$q(x,y) = q_0 \sin\frac{\pi x}{a} \sin\frac{\pi y}{b} \tag{30}$$

the following sets of displacements and transverse shear strains will satisfy the governing eqns (15):

$$\begin{aligned}
u_0^1(x,y) &= U \cos\frac{\pi x}{a} \sin\frac{\pi y}{b} \\
v_0^1(x,y) &= V \sin\frac{\pi x}{a} \cos\frac{\pi y}{b} \\
\phi_x^1(x,y) &= F_x \cos\frac{\pi x}{a} \sin\frac{\pi y}{b} \\
\phi_y^1(x,y) &= F_y \sin\frac{\pi x}{a} \cos\frac{\pi y}{b} \\
w(x,y) &= W \sin\frac{\pi x}{a} \sin\frac{\pi y}{b}.
\end{aligned} \tag{31}$$

Substituting eqns (30) and (31) into eqn (15) and collecting the coefficients result in five algebraic equations which can be put in matrix form as

$$\mathbf{Ax} = \mathbf{b}, \tag{32}$$

where $\mathbf{A}$ is a matrix of known coefficients, $\mathbf{x}$ is the unknown generalized displacement amplitude vector and $\mathbf{b}$ is the applied generalized load amplitude vector. These vectors are given by

$$\begin{aligned}
\mathbf{x} &= [U \quad V \quad F_x \quad F_y \quad W]^{\mathrm{T}} \\
\mathbf{b} &= [0 \quad 0 \quad 0 \quad 0 \quad q_0]^{\mathrm{T}}.
\end{aligned} \tag{33}$$

In the presentation of the results, non-dimensionalized displacements and stresses are defined in the usual manner with respect to the data as follows:

$$\begin{aligned}
\bar{u} &= \frac{E_T u}{q_0 h R^3} \\
\bar{w} &= \frac{100 E_T w}{q_0 h R^4} \\
(\bar{\sigma}_1, \bar{\sigma}_2, \bar{\sigma}_6) &= \frac{(\sigma_1, \sigma_2, \sigma_6)}{q_0 R^2} \\
(\bar{\sigma}_4, \bar{\sigma}_5) &= \frac{(\sigma_4, \sigma_5)}{q_0 R},
\end{aligned} \tag{34}$$

where $R = a/h$. Unless otherwise stated, the results for the transverse shear stress distributions $\bar{\sigma}_4$ and $\bar{\sigma}_5$ are obtained from integration through the thickness of the appropriate three-dimensional equilibrium equations of elasticity and not from the constitutive equations. Also, displacement and stress distributions through the thickness are described with respect to the non-dimensionalized thickness coordinate $\bar{z}$, that is, z/h.

The numerical results for the five problems are presented in Tables 1–5 and Figs 2–10. In the predictor phase of the present predictor-corrector approach, the linear zig-zag model has been used throughout. Only a single corrector phase is found to be necessary, and three terms are employed in the Chebyshev polynomial approximation. Table 1 gives the values of the non-dimensionalized stresses through the thickness of the (0°/90°) square laminate of Problem (1) for a/h of 4. It is seen that the present results are closer to the exact elasticity results than the DST and LT. This can be observed by considering the values of the stress component $\bar{\sigma}_1$ for $a/h = 4$ at the free surfaces and at the interfaces given in Table 1. For the 0° layer, the present results are in error by a negligible 1.1% at both $\bar{z} = -0.5$ and $\bar{z} = 0.0$ whereas those for the DST are in error by 3.5 and 23%, respectively. The results from the LT are even less accurate for this problem with errors of 18 and 20%, respectively. At the free surface of the 90° layer, the prediction for $\bar{\sigma}_1$ (although much smaller than at

Table 1. Nondimensionalized stresses in (0°/90°) square laminate under sinusoidal loading ($t = h/2$, $a = b$, $a/h = 4$)

$\bar{z}$	Source	$\bar{\sigma}_1$	$\bar{\sigma}_2$	$\bar{\sigma}_4$	$\bar{\sigma}_5$	$\bar{\sigma}_6$
−0.50	Pagano	−0.7807	−0.0955	0.0000	0.0000	0.0591
	Present	−0.7894	−0.1054	0.0000	0.0000	0.0640
	Lee *et al.*	−0.9176	−0.0702	0.0000	0.0000	0.0485
	Di Sciuva	−0.8078	−0.0634	0.0000	0.0000	0.0591
−0.40	Pagano	−0.3988	−0.0734	0.0423	0.1976	0.0427
	Present	−0.3807	−0.0823	0.0466	0.1956	0.0464
	Lee *et al.*	−0.5148	−0.0520	0.0318	0.2362	0.0335
	Di Sciuva	−0.5017	−0.0551	0.0309	0.2180	0.0348
−0.30	Pagano	−0.1437	−0.0553	0.0738	0.2919	0.0307
	Present	−0.1312	−0.0635	0.0818	0.2855	0.0338
	Lee *et al.*	−0.1643	−0.0395	0.0547	0.3504	0.0220
	Di Sciuva	−0.1957	−0.0468	0.0565	0.3371	0.0261
−0.20	Pagano	0.0598	−0.0398	0.0968	0.3127	0.0209
	Present	0.0523	−0.0474	0.1080	0.3062	0.0227
	Lee *et al.*	0.1471	−0.0311	0.0712	0.3577	0.0132
	Di Sciuva	0.1104	−0.0385	0.0767	0.3574	0.0174
−0.10	Pagano	0.2792	−0.0258	0.1122	0.2659	0.0117
	Present	0.2628	−0.0327	0.1260	0.2641	0.0122
	Lee *et al.*	0.4324	−0.0255	0.0830	0.2690	0.0062
	Di Sciuva	0.4164	−0.0302	0.09162	0.2787	0.0087
0.00	Pagano	0.5872	−0.0122	0.1202	0.1353	0.0012
	Present	0.5934	−0.0179	0.1360	0.1360	0.0000
	Lee *et al.*	0.7046	−0.0214	0.0913	0.0913	0.0000
	Di Sciuva	0.7225	−0.0219	0.1012	0.1012	0.0000
0.00^{+}	Pagano	0.0247	−0.6307	0.1202	0.1353	0.0012
	Present	0.0179	−0.5934	0.1360	0.1360	0.0000
	Lee *et al.*	0.0213	−0.7046	0.0913	0.0913	0.0000
	Di Sciuva	0.0219	−0.7225	0.1012	0.1012	0.0000
0.10	Present	0.0327	−0.2628	0.2641	0.1260	−0.0123
	Present	0.0327	−0.2628	0.2641	0.1260	−0.0123
	Lee *et al.*	0.0255	−0.4324	0.2691	0.0830	−0.0062
	Di Sciuva	0.0302	−0.4164	0.2787	0.0916	−0.0087
0.20	Pagano	0.0508	−0.0789	0.3188	0.1063	−0.0188
	Present	0.0474	−0.0523	0.3062	0.1079	−0.0227
	Lee *et al.*	0.0311	−0.1471	0.3577	0.0712	−0.0132
	Di Sciuva	0.0385	−0.1104	0.3574	0.0767	−0.0174
0.30	Pagano	0.0667	0.1387	0.3027	0.0807	−0.0282
	Present	0.0635	0.1312	0.2855	0.0818	−0.0334
	Lee *et al.*	0.0396	0.1643	0.3504	0.0547	−0.0220
	Di Sciuva	0.0468	0.1957	0.3371	0.0565	−0.0261
0.40	Pagano	0.0859	0.4152	0.2075	0.0461	−0.0410
	Present	0.0823	0.3807	0.1956	0.0467	−0.0464
	Lee *et al.*	0.0520	0.5148	0.2363	0.0318	−0.0335
	Di Sciuva	0.0551	0.5017	0.2180	0.0309	−0.0348
0.50	Pagano	0.1098	0.8417	0.0000	0.0000	−0.0588
	Present	0.1054	0.7894	0.0000	0.0000	−0.0640
	Lee *et al.*	0.0702	0.9176	0.0000	0.0000	−0.0485
	Di Sciuva	0.0634	0.8078	0.0000	0.0000	−0.0435

$\bar{\sigma}_1 = \bar{\sigma}_1(a/2, b/2, \bar{z})$; $\bar{\sigma}_2 = \bar{\sigma}_2(a/2, b/2, \bar{z})$

$\bar{\sigma}_4 = \bar{\sigma}_4(a/2, 0, \bar{z})$; $\bar{\sigma}_5 = \bar{\sigma}_5(0, b/2, \bar{z})$; $\bar{\sigma}_6 = \bar{\sigma}_6(0, 0, \bar{z})$.

Table 2. Nondimensionalized deflections and stresses in (0°/90°/0°) square laminate under sinusoidal loading ($t = h/3$, $a = b$)

a/h	Source	$\bar{w}$	$\bar{\sigma}_1$	$\bar{\sigma}_2$	$\bar{\sigma}_4$	$\bar{\sigma}_5$	$\bar{\sigma}_6$
4	Pagano	2.006	0.801	0.534	0.2172	0.256	0.0505
	Present	2.0368	0.8003	0.5463	0.2127	0.2540	0.0531
	Lee *et al.*	1.9548	0.8443	0.6085	0.2336	0.2390	0.0504
	Di Sciuva	1.8910	0.6197	0.6607	0.2542	0.2620	0.0447
10	Pagano	0.753	0.590	0.285	0.1228	0.357	0.0289
	Present	0.7555	0.5932	0.2866	0.1220	0.3576	0.0291
	Lee *et al.*	0.7529	0.5955	0.2934	0.1243	0.3561	0.0290
	Di Sciuva	0.7233	0.5489	0.2891	0.1230	0.3643	0.0274
50	Pagano		0.541	0.185	0.0842	0.393	0.0216
	Present	0.4452	0.5410	0.1846	0.0842	0.3934	0.0216
	Lee *et al.*	0.4451	0.5411	0.1847	0.0843	0.3934	0.0216
	Di Sciuva	0.4436	0.5391	0.1843	0.0841	0.3938	0.0216
100	Pagano	0.435	0.539	0.181	0.0828	0.395	0.0216
	Present	0.4347	0.5393	0.1808	0.0828	0.3947	0.0216
	Lee *et al.*	0.4347	0.5393	0.1809	0.0828	0.3947	0.0214
	Di Sciuva	0.4343	0.5388	0.1808	0.0828	0.3948	0.0214
	CPT	0.4312	0.539	0.180	0.0823	0.395	0.0213

$\bar{w} = \bar{w}(a/2, b/2, \bar{z})$; $\bar{\sigma}_1 = \bar{\sigma}_1(a/2, b/2, 1/2)$; $\bar{\sigma}_2 = \bar{\sigma}_2(a/2, b/2, 1/6)$
$\bar{\sigma}_4 = \bar{\sigma}_4(a/2, 0, 0)$; $\bar{\sigma}_5 = \bar{\sigma}_5(0, b/2, 0)$; $\bar{\sigma}_6 = \bar{\sigma}_6(0, 0, -1/2)$.

Table 3. Nondimensionalized deflections and stresses in (0°/90°/0°) rectangular laminate under sinusoidal loading ($t = h/3$, $b = 3a$)

a/h	Source	$\bar{w}$	$\bar{\sigma}_1$	$\bar{\sigma}_2$	$\bar{\sigma}_4$	$\bar{\sigma}_5$	$\bar{\sigma}_6$
4	Pagano	2.82	1.14	0.109	0.0334	0.351	0.0281
	Present	2.8424	1.1431	0.1119	0.0315	0.3469	0.0279
	Lee *et al.*	2.7395	1.2069	0.1082	0.0301	0.3273	0.0276
	Di Sciuva	2.7172	0.9251	0.1138	0.0318	0.3658	0.0255
10	Pagano	0.919	0.726	0.0418	0.0152	0.420	0.0123
	Present	0.9205	0.7277	0.0420	0.0149	0.4198	0.0122
	Lee *et al.*	0.9185	0.7314	0.0420	0.0148	0.4186	0.0122
	Di Sciuva	0.8810	0.6746	0.0410	0.0147	0.4269	0.0115
50	Pagano	0.520	0.628	0.0259	0.0110	0.439	0.0084
	Present	0.5205	0.6277	0.0258	0.0110	0.4387	0.0084
	Lee *et al.*	0.5205	0.6277	0.0258	0.0110	0.4387	0.0084
	Di Sciuva	0.5187	0.6253	0.0258	0.0109	0.4390	0.0084
100	Pagano	0.508	0.624	0.0253	0.0108	0.439	0.0083
	Present	0.5077	0.6244	0.0253	0.0108	0.4393	0.0083
	Lee *et al.*	0.5077	0.6244	0.0253	0.0108	0.4394	0.0083
	Di Sciuva	0.5070	0.6240	0.0253	0.0108	0.4394	0.0083
	CPT	0.503	0.623	0.0252	0.0108	0.440	0.0083

$\bar{w} = \bar{w}(a/2, b/2, \bar{z})$; $\bar{\sigma}_1 = \bar{\sigma}_1(a/2, b/2, 1/2)$; $\bar{\sigma}_2 = \bar{\sigma}_2(a/2, b/2, 1/6)$
$\bar{\sigma}_4 = \bar{\sigma}_4(a/2, 0, 0)$; $\bar{\sigma}_5 = \bar{\sigma}_5(0, b/2, 0)$; $\bar{\sigma}_6 = \bar{\sigma}_6(0, 0, -1/2)$.

the other free surface) using the present approach is different from the exact elasticity value by only 4.0% while those from the DST and the LT are off by a huge margin of 42 and 36%, respectively. Similar observations can be made for the stress component $\bar{\sigma}_2$ which behaves basically in the same manner as $\bar{\sigma}_1$ but in the opposite z direction.

Figures 2 and 3 depict the distributions of $\bar{\sigma}_1(a/2, b/2, \bar{z})$ and $\bar{\sigma}_5(0, b/2, \bar{z})$ across the thickness of the laminate of Problem (1) obtained from exact elasticity, the present theory, the DST and the LT for $a/h = 4$. It is seen that the results from the present theory follow the curves from exact elasticity much more closely than the others. This is most obvious in Fig. 3 for the transverse shear stress $\bar{\sigma}_5$ which shows substantial differences between exact elasticity and the DST and LT. The maximum value of $\bar{\sigma}_5$ occurs near $\bar{z} = -0.2$. At this location, it can be deduced from Table 1 that the value of $\bar{\sigma}_5$ from the present theory is off by only 2.1% while those from both the DST and LT are in error by as much as 14%.

The variation of the maximum deflection $\bar{w}(a/2, b/2, 0)$ with a/h is plotted in Fig. 4 for the different theories. The figure shows that the present predictor-corrector approach gives practically the same solution as exact elasticity over the range of a/h from 4 to 100. The

Table 4. Nondimensionalized deflections and stresses in (0°/90°/90°/0°) square laminate under sinusoidal loading ($t = h/4$, $a = b$)

a/h	Source	$\bar{w}$	$\bar{\sigma}_1$	$\bar{\sigma}_2$	$\bar{\sigma}_4$	$\bar{\sigma}_5$	$\bar{\sigma}_6$
4	Pagano	1.9367	0.720	0.663	0.292	0.219	0.0467
	Present	1.9646	0.7155	0.6766	0.2883	0.2183	0.0487
	Lee *et al.*	1.8514	0.7272	0.7182	0.3292	0.2063	0.0418
	Di Sciuva	1.6888	0.5239	0.8035	0.3746	0.2035	0.0351
10	Pagano	0.7370	0.559	0.401	0.196	0.301	0.0275
	Present	0.7394	0.5611	0.4023	0.1954	0.3016	0.0277
	Lee *et al.*	0.7313	0.5609	0.4111	0.2015	0.2992	0.0273
	Di Sciuva	0.7068	0.5220	0.4164	0.2048	0.3013	0.0261
50	Pagano	0.4446	0.539	0.276	0.141	0.337	0.0216
	Present	0.4447	0.5394	0.2760	0.1411	0.3373	0.0216
	Lee *et al.*	0.4448	0.5394	0.2763	0.1413	0.3373	0.0216
	Di Sciuva	0.4434	0.5378	0.2762	0.1413	0.3375	0.0215
100	Pagano	0.4347	0.539	0.271	0.139	0.339	0.0214
	Present	0.4346	0.5389	0.2710	0.1390	0.3388	0.0214
	Lee *et al.*	0.4346	0.5389	0.2711	0.1390	0.3388	0.0214
	Di Sciuva	0.4343	0.5387	0.2708	0.1390	0.3388	0.0213
	CPT	0.4312	0.539	0.269	0.138	0.339	0.0213

$\bar{w} = \bar{w}(a/2, b/2, \bar{z})$; $\bar{\sigma}_1 = \bar{\sigma}_1(a/2, b/2, 1/2)$; $\bar{\sigma}_2 = \bar{\sigma}_2(a/2, b/2, 1/4)$
$\bar{\sigma}_4 = \bar{\sigma}_4(a/2, 0, 0)$; $\bar{\sigma}_5 = \bar{\sigma}_5(0, b/2, 0)$; $\bar{\sigma}_6 = \bar{\sigma}_6(0, 0, -1/2)$.

Table 5. Nondimensionalized deflections and stresses in (0°/90°/0°/90°/0°) square laminate under sinusoidal loading ($t = h/6$, $a = b$)

a/h	Source	$\bar{w}$	$\bar{\sigma}_1$	$\bar{\sigma}_2$	$\bar{\sigma}_4$	$\bar{\sigma}_5$	$\bar{\sigma}_6$
4	Pagano	1.8505	0.685	0.663	0.229	0.238	0.0394
	Present	1.8753	0.6747	0.6571	0.2254	0.2362	0.0408
	Lee *et al.*	1.8151	0.6910	0.6241	0.2406	0.2298	0.0357
	Di Sciuva	1.5599	0.4926	0.6582	0.3084	0.2117	0.0242
10	Pagano	0.6771	0.545	0.430	0.223	0.258	0.0246
	Present	0.6795	0.5475	0.4320	0.2231	0.2582	0.0247
	Lee *et al.*	0.6689	0.5469	0.4302	0.2278	0.2557	0.0241
	Di Sciuva	0.6269	0.5397	0.4050	0.2275	0.2546	0.0235
50	Pagano	0.4412	0.539	0.363	0.206	0.271	0.0214
	Present	0.4414	0.5387	0.3627	0.2064	0.2715	0.0214
	Lee *et al.*	0.4410	0.5386	0.3627	0.2066	0.2713	0.0214
	Di Sciuva	0.4399	0.5368	0.3636	0.2073	0.2710	0.0214
100	Pagano	0.4338	0.539	0.360	0.205	0.272	0.0213
	Present	0.4338	0.5387	0.3600	0.2055	0.2720	0.0213
	Lee *et al.*	0.4337	0.5387	0.3600	0.2056	0.2720	0.0213
	Di Sciuva	0.4332	0.5386	0.3598	0.2055	0.2720	0.0213
	CPT	0.4312	0.539	0.359	0.205	0.272	0.0213

$\bar{w} = \bar{w}(a/2, b/2, \bar{z})$; $\bar{\sigma}_1 = \bar{\sigma}_1(a/2, b/2, 1/2)$; $\bar{\sigma}_2 = \bar{\sigma}_2(a/2, b/2, 1/3)$
$\bar{\sigma}_4 = \bar{\sigma}_4(a/2, 0, 0)$; $\bar{\sigma}_5 = \bar{\sigma}_5(0, b/2, 0)$; $\bar{\sigma}_6 = \bar{\sigma}_6(0, 0, -1/2)$.

results from the DST and LT can be different from the exact elasticity solution by as much as 20% for small values of a/h. It can be concluded that the present approach has improved the results of the DST and LT significantly through the use of a general higher-order zig-zag model in the corrector phase.

The results for the (0°/90°/0°) square and rectangular laminates of Problems (2) and (3) at different values of a/h ranging from 4 to 100 are presented in Tables 2 and 3. While the LT can provide a fairly accurate solution for these two problems, the present method gives results which are even closer to exact elasticity. For instance, at $a/h = 4$ for the square laminate, the value of $\bar{\sigma}_1$ at $(a/2, b/2, 1/2)$ is only 0.1% from the exact elasticity value while those from the DST and LT are different by 23 and 5.4%, respectively. For the rectangular laminate, these differences are 0.3, 19 and 5.9%, respectively.

The distributions of the displacements and stresses through the thickness for the square laminate are shown in Figs 5–8 for exact elasticity and the three zig-zag models. It is clear that while the LT can give accurate results for the maximum in-plane displacement $\bar{u}$ and in-plane stress $\bar{\sigma}_1$ which occur at the free surfaces, only the present model produces results

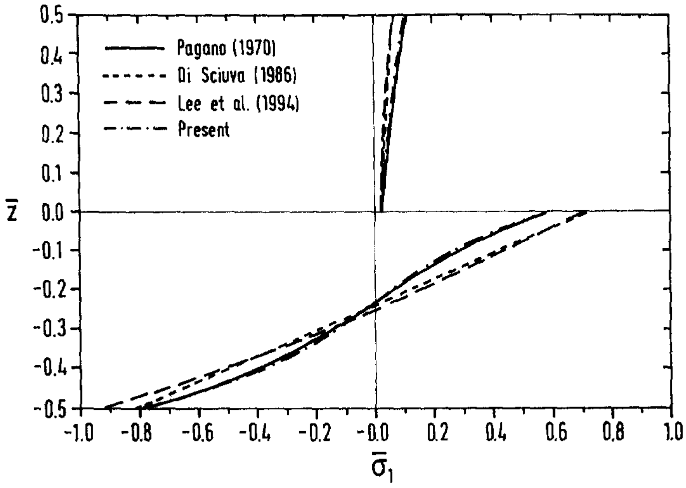

Fig. 2. Distribution of in-plane stress $\bar{\sigma}_1(a/2, b/2, \bar{z})$ in a (0°/90°) square laminate with $a/h = 4$ under sinusoidal loading.

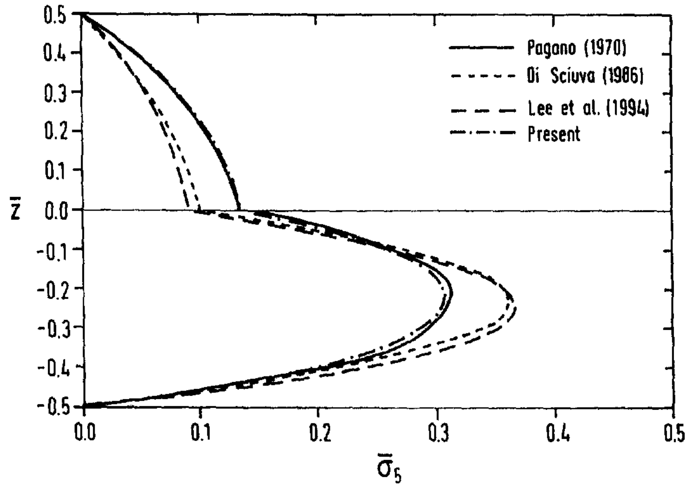

Fig. 3. Distribution of transverse shear stress $\bar{\sigma}_5(0, b/2, \bar{z})$ in a (0°/90°) square laminate with $a/h = 4$ under sinusoidal loading.

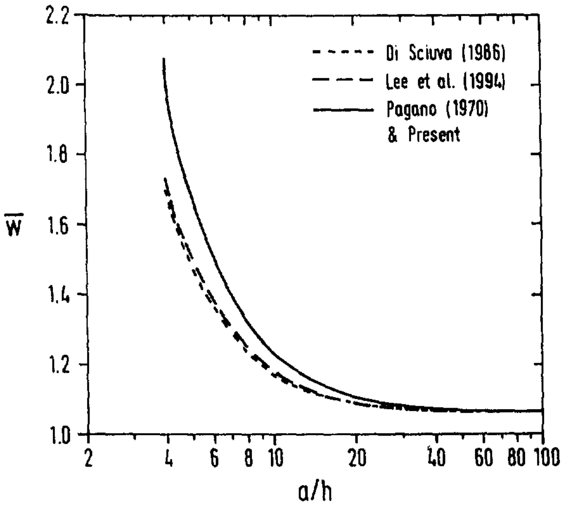

Fig. 4. Variation of maximum deflection $\bar{w}(a/2, b/2, 0)$ with a/h in a (0°/90°) square laminate with $a/h = 4$ under sinusoidal loading.

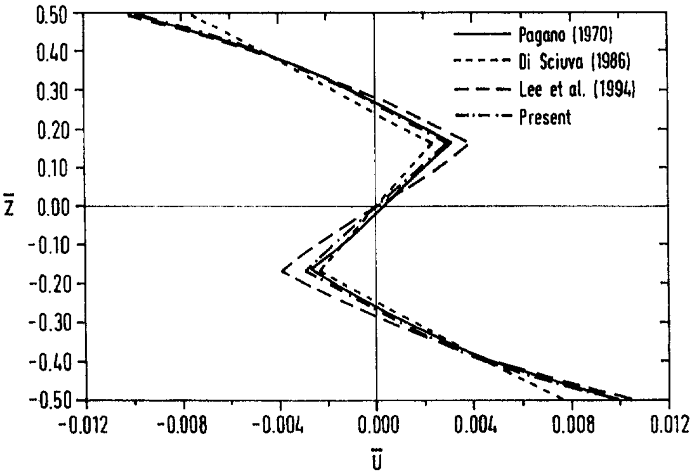

Fig. 5. Distribution of in-plane displacement $\bar{u}(0, b/2, \bar{z})$ in a $(0°/90°/0°)$ square laminate with $a/h = 4$ under sinusoidal loading.

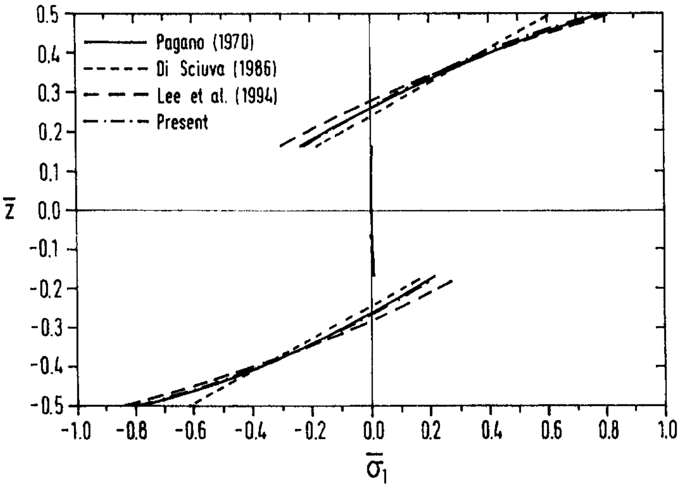

Fig. 6. Distribution of in-plane stress $\bar{\sigma}_1(a/2, b/2, \bar{z})$ in a $(0°/90°/0°)$ square laminate with $a/h = 4$ under sinusoidal loading.

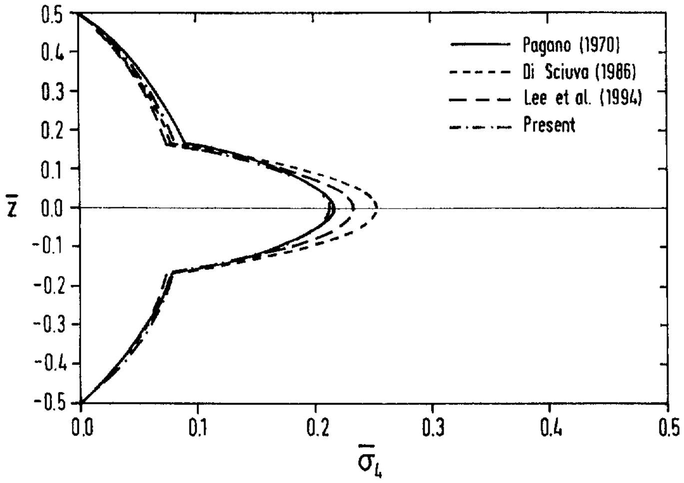

Fig. 7. Distribution of transverse shear stress $\bar{\sigma}_4(a/2, 0, \bar{z})$ in a $(0°/90°/0°)$ square laminate with $a/h = 4$ under sinusoidal loading.

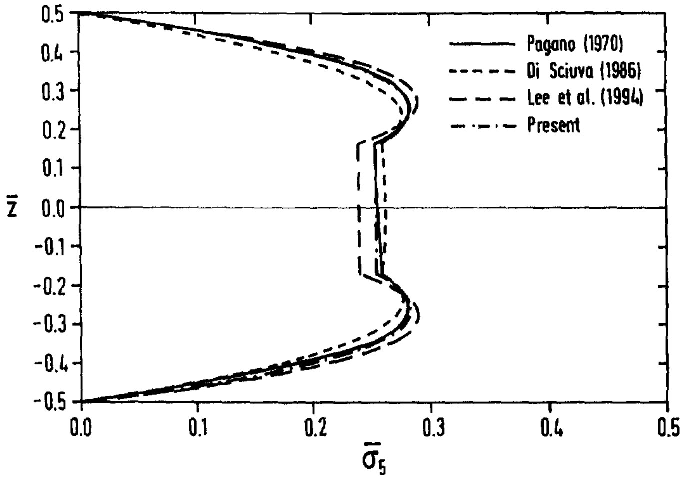

Fig. 8. Distribution of transverse shear stress $\sigma_5(0, b/2, \bar{z})$ in a (0°/90°/0°) square laminate with $a/h = 4$ under sinusoidal loading.

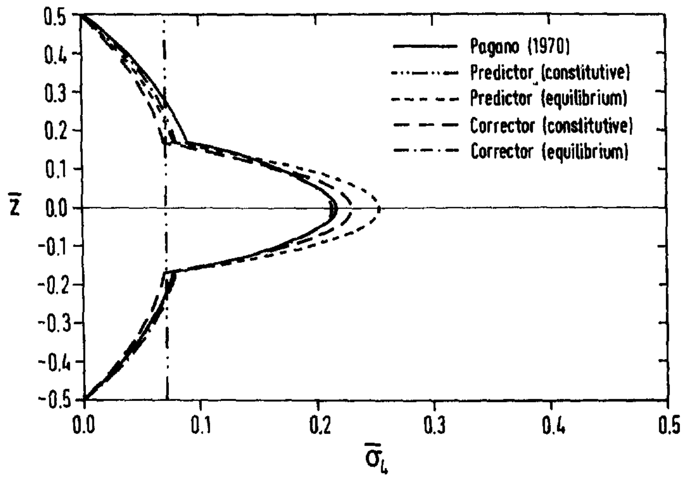

Fig. 9. Change in distribution of transverse shear stress $\sigma_4(a/2, 0, \bar{z})$ in a (0°/90°/0°) square laminate with $a/h = 4$ under sinusoidal loading during different stages of predictor–corrector approach.

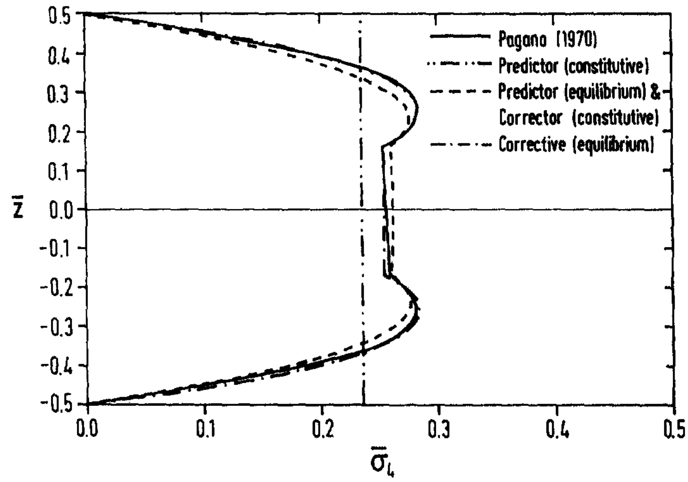

Fig. 10. Change in distribution of transverse shear stress $\sigma_5(0, b/2, \bar{z})$ in a (0°/90°/0°) square laminate with $a/h = 4$ under sinusoidal loading during different stages of predictor–corrector approach.

which are accurate throughout the thickness of the laminate, including the locations at the interfaces. This is also true of the transverse shear stresses $\bar{\sigma}_4$ and $\bar{\sigma}_5$, especially in the 90° layer.

As explained earlier, the present approach relies on the predictor phase to supply a good estimate of the transverse shear stress distributions for the determination of the functions $f_x^k(z)$ and $f_y^k(z)$ in the general higher-order displacement field of the corrector phase. The changes in the distributions of $\bar{\sigma}_4$ and $\bar{\sigma}_5$ at the various stages of the present approach are illustrated in Figs 9 and 10, respectively. Starting from the uniform distribution provided by the constitutive equations in the predictor phase using the linear zig-zag model, the shear stresses take on an improved distribution through the use of the equilibrium equations in the predictor phase. The fact that the distributions from the constitutive and equilibrium calculations are vastly different from each other at this stage is an indication of possible inaccuracies in the solution for the displacements and stresses in the predictor phase. The shapes but not the actual magnitudes of the improved distribution are then used in the corrector phase for the calculation of the new solution. The accuracy of this solution can be ascertained from a comparison of the distributions from the constitutive and equilibrium calculations in the corrector phase. These distributions are observed to be quite close to each other in the present problem, thus indicating the reliability of the solution in the corrector phase.

The results for the (0°/90°/90°/0°) and (0°/90°/0°/90°/0°) square laminates in the last two problems are listed in Tables 4 and 5. An examination of the tables confirms that the present approach behaves equally well for these two problems.

CONCLUSIONS

A new predictor–corrector approach based on the use of a general higher-order layerwise displacement model was presented. This higher-order model included the linear and cubic zig-zag models as special cases. In the predictor phase, one of the latter two models was employed for the purpose of obtaining a good estimate of the transverse shear stress distributions through the use of the equilibrium equations of elasticity. With this estimate, the polynomial functions for the layerwise displacement field in the corrector phase were deduced. For multiple corrector phases, it was shown that Chebyshev polynomials could be used to determine the polynomial functions effectively.

Five standard test problems on the bidirectional bending of both symmetric and antisymmetric thick laminates were solved with the proposed approach. The numerical results were found to be in excellent agreement with the exact elasticity results of Pagano for laminates with length-to-thickness ratios of as low as 4. There was a significant improvement over the results from the linear and cubic zig-zag models especially at the interfaces. The results also confirmed that the inaccuracies in such models were due entirely to the differences between the assumed shape of the transverse shear stresses provided by the constitutive equations and the calculated shape of the same stresses from the equilibrium equations of elasticity. Minimising these differences was the central objective of the present predictor–corrector zig-zag model.

REFERENCES

Ambartsumyan, S. A. (1969). *Theory of Anisotropic Plates*. Technomic Publishing Co. Stamford, Conn.

Chou, P. C. and Carleone, J. (1973). Transverse shear in laminated plate theories. *AIAA J.* **11**, 1333–1336.

Di Sciuva, M. (1986). Bending, vibration and buckling of simply supported thick multilayered orthotropic plates: An evaluation of a new displacement model. *J. Sound Vibr.* **105**, 425–442.

Lee, K. H., Senthilnathan, N. R., Lim, S. P. and Chow, S. T. (1990). An improved zig-zag model for the bending of laminated composite plates. *Compos. Structures* **15**, 137–148.

Lee, K. H., Lin, W. Z. and Chow, S. T. (1994). Bidirectional bending of laminated composite plates using an improved zig-zag model. *Compos. Structures* **28**, 283–294.

Mau, S. T. (1973). A refined laminated plate theory. *J. Appl. Mech.* **40**, 606–607.

Murakami, H. (1986). Laminated composite plate theory with improved in-plane responses. *J. Appl. Mech.* **53**, 661–666.

Noor, A. K. and Burton, W. S. (1989). Stress and free vibration analyses of multilayered composite plates. *Comp. Structures* **11**, 183–204.

Noor, A. K. and Peters, J. M. (1989). *A posteriori* estimates for shear correction factors in multi-layered composite cylinders. *J. Engng Mech.* **115**, 1225–1244.

Noor, A. K., Burton, W. S. and Peters, J. M. (1990). Predictor-corrector procedures for stress and free vibration analyses of multilayered composite plates and shells. *Comp. Meth. Appl. Mech. Engng* **82**, 341–363.

Noor, A. K., Burton, W. S. and Peters, J. M. (1991). Assessment of computational models for multilayered composite cylinders. *Int. J. Solids Structures* **27**, 1269–1286.

Pagano, N. J. (1969). Exact solutions for composite laminates in cylindrical bending. *J. Comp. Mat.* **3**, 398–411.

Pagano, N. J. (1970). Exact solutions for rectangular bidirectional composites and sandwich plates. *J. Comp. Mat.* **4**, 20–34.

Pagano, N. J. and Hatfield, S. J. (1972). Elastic behavior of multilayered bidirectional composites. *AIAA J.* **10**, 931–933.

Reddy, J. N. (1987). A generalization of two-dimensional theories of laminated composite plates. *Commun. Appl. Numer. Meth.* **3**, 173–180.

Reddy, K. J., Nagaraja, K. S. and Vijayakumar, K. (1991). New approach for the analysis of flexure of symmetric laminates. *AIAA J.* **29**, 1960–1966.

Ren, J. G. (1986). A new theory of laminated plate. *Comp. Sci. Technol.* **26**, 225–239.

Whitney, J. M. (1969). The effect of transverse shear deformation on the bending of laminated plates. *J. Comp. Mat.* **3**, 534–547.